

Ozonation of *Para*-Substituted Phenolic Compounds Yields *p*-Benzoquinones, Other Cyclic α,β -Unsaturated Ketones, and Substituted Catechols

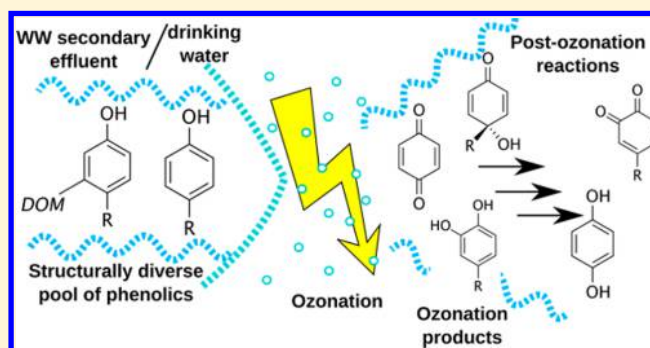
Peter R. Tentscher,[†] Marc Bourgin,[†] and Urs von Gunten^{*,†,‡}

[†]Eawag, Swiss Federal Institute of Aquatic Science and Technology, Ueberlandstrasse 133, 8600 Duebendorf, Switzerland

[‡]School of Architecture, Civil and Environmental Engineering (ENAC), École Polytechnique Fédérale de Lausanne (EPFL), 1015, Lausanne, Switzerland

S Supporting Information

ABSTRACT: Phenolic moieties are common functional groups in organic micropollutants and in dissolved organic matter, and are exposed to ozone during drinking water and wastewater ozonation. Although unsubstituted phenol is known to yield potentially genotoxic *p*-benzoquinone during ozonation, little is known about the effects of substitution of the phenol ring on transformation product formation. With batch experiments employing differing ozone/target compound ratios, it is shown that *para*-substituted phenols (*p*-alkyl, *p*-halo, *p*-cyano, *p*-methoxy, *p*-formyl, *p*-carboxy) yield *p*-benzoquinones, *p*-substituted catechols, and 4-hydroxy-4-alkyl-cyclohexadien-1-ones as common ozonation products. Only in a few cases did *para*-substitution prevent the formation of these potentially harmful products. Quantum chemical calculations showed that different reaction mechanisms lead to *p*-benzoquinone, and that cyclohexadienone can be expected to form if no such pathway is possible. These products can thus be expected from most phenolic moieties. Kinetic considerations showed that substitution of the phenolic ring results in rather small changes of the apparent second order rate constants for phenol–ozone reactions at pH 7. Thus, in mixtures, most phenolic structures can be expected to react with ozone. However, redox cross-reactions between different transformation products, as well as hydrolysis, can be expected to further alter product distributions under realistic treatment scenarios.



INTRODUCTION

Ozone (O_3) has been applied as a disinfectant/oxidant for drinking water treatment for the last 100 years,¹ and ozonation has been recently considered and implemented for the abatement of organic micropollutants in secondary wastewater effluents.^{2–6} O_3 mainly reacts with micropollutants containing electron-rich moieties (activated aromatics, olefins, aliphatic amines, thioethers) that compete with dissolved organic matter (DOM) for the dosed O_3 .^{1,7} For typical ozonation conditions, mineralization of organic compounds does generally not occur.⁸ This may lead to potentially toxic transformation products from the reactions of ozone with both micropollutants and DOM.

Biologically active chemicals such as pharmaceuticals generally lose their activity (e.g., estrogenicity, antimicrobial activity, etc.) upon small structural changes such as those induced by a primary reaction with an oxidant.^{9–16} However, oxidation can yield electrophilic compounds (e.g., *p*-benzoquinones, α,β -unsaturated carbonyls, peroxides, radicals), which can oxidize cell constituents, for example, by covalent addition to electron-rich moieties (thiols, amines) or by electron-transfer reactions. For example, a thiol group of a biomolecule can undergo a Michael-addition to an α,β -unsaturated carbonyl.

Such reactions can lead to cytotoxic effects or, in the case of reaction with DNA moieties, to genotoxicity.¹⁷

We examined structural alerts for carcinogenic functional groups,¹⁸ the carcinogenic potency project,^{19–21} and compared these carcinogenic moieties to published literature on O_3 transformation pathways.¹ We derived that ozonation of phenolic compounds can lead to rodent carcinogens (electrophilic *p*-benzoquinones, but also to electron-rich hydroquinones and catechols).¹⁹ Of these, *p*-benzoquinone (but not the dihydroxybenzenes) is also part of the set of structural alerts for carcinogenicity. These transformation products were detected in detailed product studies performed on (unsubstituted) phenol, which also identified ring-opening products as further transformation products.^{22,23}

Phenolic structures are common moieties in many micropollutants: a list of currently 563 surface water micropollutants based on ref 24 contains 35 substances with phenolic

Received: January 2, 2018

Revised: February 26, 2018

Accepted: March 1, 2018

Published: March 21, 2018

moieties,²⁴ and more can be formed as primary products from ozone/hydroxyl radical ($\bullet\text{OH}$) attack of nonphenolic aromatics.^{1,25,26} The content of oxidizable phenols in fulvic acid is between 2.3 and 2.9 mmol phenol/g C,²⁷ and wastewater effluent DOM may contain ~45% fulvic acid.²⁸ At a DOM concentration of 10 mg/L, this would result in a phenol concentration of ~10–13 μM , significantly higher than the concentrations of phenolic/aromatic moieties in micropollutants.

The combined pool of phenolic compounds is structurally diverse, with different substituents on the phenolic ring in all positions. The formation of *p*-benzoquinones and hydroquinones requires an attack of O_3 in the *para* position, and substitution of the parent compound in this position may prevent their formation. In contrast, ortho-attack may lead to the formation of catechols, and ortho-substitution may prevent their formation. A few product studies have been performed so far for ozone reactions with *p*-substituted phenols:

For hydroquinone,²³ bisphenol A,²⁹ *t*-butyl-4-hydroxyanisole,³⁰ *p*-chlorophenol,³¹ and 2,4-dichlorophenol,³² (substituted) *p*-benzoquinones were reported as products. In contrast, hydroquinone was reported as a product of unsubstituted phenol (in low concentration), paracetamol,³³ and *p*-chlorophenol,³⁴ and *t*-butyl-hydroquinone for *t*-butyl-4-hydroxyanisole.³⁰ Substituted catechols were found in ozonated samples of bisphenol A,³³ *t*-butyl-4-hydroxyanisole,³⁰ *p*-chlorophenol,^{31,34} paracetamol,³³ and 4-alkylphenols.³⁵ In contrast, ozonation of (unsubstituted) catechol yielded ring-opening products.^{23,36}

In these studies, $\bullet\text{OH}$, formed during ozonation of phenolic compounds³⁷ was not always quenched and product yields were frequently not determined. Therefore, these studies do not allow for general conclusions on the type of parent phenols that yield *p*-benzoquinone, hydroquinone, or similar compounds. This warrants a systematic investigation of substituent effects on yields of these potentially harmful products. Ultimately, it is desirable to predict potential product structures from the parent structure, which requires well-defined reaction rules based on mechanistic insights.³⁸

The aim of the present study was to investigate how substitution of phenolic compounds impacts product formation, with a special focus on potentially genotoxic products. A set of structurally simple phenolic model compounds was selected, with a focus on *para*-substitution, which was expected to have the largest influence on product distribution. These compounds were ozonated in batch experiments with varying molar O_3 /target compound ratios, and products in the reaction mixtures at pH 3 and pH 7 were identified and quantified with high performance liquid chromatography (HPLC) coupled to a diode array detector (DAD) and in some cases coupled to a high resolution mass spectrometer (HRMS).

MATERIALS AND METHODS

Standards and Reagents. A list of chemicals, suppliers, and purities of the selected compounds is provided in the Supporting Information (SI) (Table S1).

Ozonation Batch Experiments. To determine yields of transformation products from the ozone reactions with the selected phenols, room temperature phenol reaction solutions (pH 3 and pH 7) were spiked with different volumes of a room temperature ozone stock solution, yielding molar ratios of O_3 to substrate of ~0.125 to ~1.75. $\bullet\text{OH}$ was scavenged with *t*-BuOH. Phenol starting concentrations were 100 μM for the

quantification of organic oxidation products and 400 μM for the quantification of H_2O_2 . Details are given in section S0.2.

Analytical Methods. HPLC-DAD Analysis. Parent phenols, (substituted) catechols, hydroquinone, (substituted) *p*-benzoquinone and 4-hydroxy-4-(methyl/ethyl)cyclohexadien-1-one were quantified using external standards. All analyses were carried out on an Agilent 1100 with a photodiode array detector. The HPLC protocol is described in section S0.3.

H_2O_2 in the reaction mixtures was quantified by singlet oxygen production of the reaction of H_2O_2 with HOCl .^{39,40} Details are given in section S0.3.

LC-HRMS Analysis of the *p*-Me-Phenol Reaction Mixtures. After ozonation, samples were transferred to amber vials for LC-HRMS analysis without sample pretreatment. Details are described in section S0.3.

Quantum Chemical Calculations. Density functional theory (DFT) calculations were performed with Gaussian09, revision D01. Standard settings of this software package were used unless specified otherwise. Reaction pathway calculations used the M062x⁴¹ functional, QSAR descriptors the M11⁴² functional, and additional calculations used the CBS-QB3⁴³ method. More details are given in sections S0.4 and S1.1.

RESULTS AND DISCUSSION

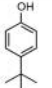
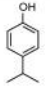
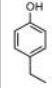
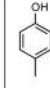

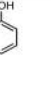
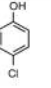
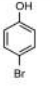
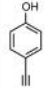
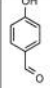
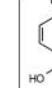


Choice of Model Compounds. The chemical structures and (estimated) physicochemical parameters of the compounds selected for ozonation experiments are shown in Table 1. Most of them are *para*-substituted, which is expected to influence the yield of *p*-oxygenated products (*p*-benzoquinone, hydroquinone). To cover the structural diversity found in micropollutants²⁴ and natural DOM,⁴⁴ substituents differ in steric demand and electronic (de)activation of the aromatic ring.

For the unsubstituted phenol, the contribution of the different species (phenol/phenolate) to the observed reactivity with O_3 at a given pH can be calculated from the $\text{p}K_a$ and the species-specific second order rate constants.¹ Kinetically, phenolate is the dominant ozone-reactive species at pH > 4, and the only relevant species at pH 7, whereas phenol is the dominant species reacting with ozone at pH 3. Considering the second order rate constants in Table 1, this assumption generally holds across the set of substituted phenols for pH 7, with the exception of the most activated systems (e.g., 4-methoxyphenol). For pH 3, a significant contribution of the phenolates is possible if the $\text{p}K_a$ is low enough. For 2,6-dibromophenol, the phenolate should even be the only relevant ozone-reactive species at pH 3.

Although it could be expected that deactivated phenols react slower with O_3 , this effect is (partially) masked by speciation. The kinetics of ozone reactions with dissociating compounds was described by Hoigné and Bader⁴⁵ (section S1). In brief, activation of the aromatic ring (that is, positive inductive and mesomeric effects) has two effects: (1) species-specific rate constants of phenol ($k(\text{PhOH})$) and phenolate ($k(\text{PhO}^-)$) increase (2) the $\text{p}K_a$ of the phenol increases, leading to a decrease of the phenolate concentration at a given pH, and consequently to a decrease of k_{obs} at pH 7. As a result, substituent effects on k_{obs} at pH 7 are antagonistic and not intuitive; changes in k_{obs} are smaller than one might expect from the changes in $k(\text{PhO}^-)$.

Product Identification by HPLC-DAD, LC-HRMS and UV/vis Spectra. All reaction mixtures were analyzed by HPLC-DAD, and *p*-benzoquinone, *p*-substituted catechols, and hydroquinone were identified by comparison (HPLC retention

Table 1. Phenolic Model Compounds Selected for Ozonation Experiments^f

													
Nr.	1	2	3	4	5	6	7	8	9	10	11	12	13
Name	4- <i>t</i> Bu-	4- <i>i</i> Prop-	4-ethyl-	4-methyl-	phenol	4-chloro-	4-bromo-	4-cyano-	4-formyl-	4-carboxy-	4-methoxy-	2,6-dimethyl-	2,6-dibromo-
pK _a	10.14 ^a	10.3 ^c	10.0 ^b	10.3 ^b	9.98 ^a	9.38 ^a	9.17 ^b	7.95 ^a	7.61 ^b	9.45 ^c	10.21 ^a	10.6 ^b	6.67 ^d /7.5 ^c
k(PhOH)	3.6×10 ^{4c}	3.7×10 ^{4c}	4.0×10 ^{4c}	3×10 ^{4d}	1.3×10 ^{4d}	6×10 ^{4d}	3.1×10 ^{4c}	1.8×10 ^{4c}	2.6×10 ^{4c}	4.1×10 ^{4c} (2.3×10 ³) ^{c,d}	4.7×10 ^{4c}	9.88×10 ^{4d}	1.1×10 ^{4c}
k(PhO ⁻)	2.7×10 ^{9c}	2.9×10 ^{9c}	3.0×10 ^{9c}	3.2×10 ^{9c}	1.4×10 ^{9d}	6×10 ^{9d}	3.8×10 ^{9c}	2.9×10 ^{9c}	1.5×10 ^{9c}	3.5×10 ^{9c}	1.1×10 ^{10c}	5.8×10 ^{9c}	2.0×10 ^{9c}
%k(PhOH), pH 3 ^e	95-100	96-100	93-100	95-99	47-99	19-96	55-99	7-89	7-88		99-100	99-100	0-2
%k(PhO ⁻), pH 7 ^e	85-100	81-100	88-100	98-100	99-100	100	99-100	100	100	79-100	59-99	60-99	100
k(obs), pH 7	2.0×10 ^{6c}	1.4×10 ^{6c}	3.1×10 ^{6c}	1.6(1.7)×10 ^{6c}	1.5(0.83 ^c) ×10 ^{6c}	2.5(1.7 ^c) ×10 ^{6c}	2.5×10 ^{6c}	2.0×10 ^{6c}	2.9×10 ^{6c}	8.9×10 ^{6c}	7.4×10 ^{6c}	1.5×10 ^{6c}	1.4×10 ^{6c}

^aLiptak et al.⁶⁰ ^bSvobodova et al.⁶¹ ^cEstimated, see section S1 for details (d) von Sonntag and von Gunten.^{1,6,7} ^dValue in parentheses refers to a neutral carboxyl group. ^eAssuming an uncertainty of one log(k) in both rate constants, see section S1. ^fAll rate constants are second order (M⁻¹ s⁻¹). %k(PhOH) and %k(PhO⁻) refer to the fraction of O₃ reacting with phenol and phenolate, respectively, at the given pH.

times and UV/vis spectra) with commercially available standards (yields in Figure 1, discussed below). *p*-Benzoquinone was detected in all reaction mixtures, except for *p*-cyanophenol. Substituted catechol was found in most reaction mixtures, hydroquinone only in those of *p*-methoxyphenol, *p*-*tert*-butylphenol (pH 3 only), and *p*-formylphenol.

The reaction mixtures of *p*-methylphenol and deuterated isotopologues (methyl-*d*₃ or ring-*d*₄) were analyzed by LC-HRMS/MS, as alkyl substitution is often encountered in micropollutants,²⁴ and because the main product (by HPLC-DAD peak area) was neither *p*-benzoquinone nor *p*-substituted catechol. It was expected that alternative transformation products are potentially genotoxic, containing, for example, an α , β -unsaturated carbonyl group.^{18,46}

Seventeen transformation products (TPs) were detected (Table S2 and Figure S2.1), some only at either pH 3 or pH 7. The structure of four TPs could be identified with high probability, two further products were deduced from a combination of measurements with mechanistic considerations (Figure 2): (1) 4-Hydroxy-4-methylcyclohexadien-1-one (TP16) was identified by synthesis of the compound and a comparison of HPLC retention times, UV/vis spectra, and MS data (Figure S2.2). It was detected in reaction mixtures at both pH 3 and pH 7.

(2) *p*-Methyl-*o*-benzoquinone (TP17), coeluting with cyclohexadienone, was detected only at pH 7 and was identified by (a) HRMS data: addition of one oxygen and loss of two protons relative to *p*-methylphenol, loss of one deuteron at the ring (Table S2), (b) UV/vis data (Figure S3). The absorption band at ~400 nm (pH 7) is compatible with a previously reported spectrum of (unsubstituted) *o*-benzoquinone,⁴⁷ (c) an ozonation experiment with *p*-methylcatechol. In the HPLC chromatogram measured after ozonation (Figure S3), one of the two main peaks eluted at the same retention time as TP17 in the *p*-methylphenol reaction mixture, with a pronounced absorption band at ~400 nm. The band at 230 nm, which was dominant in the *p*-methylphenol reaction mixture and which can be clearly attributed to 4-hydroxy-4-methyl-cyclohexadien-1-one, was not observed. (d) Chromatograms of reaction mixtures of *p*-methylcatechol with HOCl (Figure S3), in which this peak was also formed (to a much lesser extent). As halogenation could not yield the same product as ozonation, HOCl probably reacts via electron transfer to form the *o*-

benzoquinone.⁴⁸ *p*-Methyl-*o*-benzoquinone was also detected in standard solutions of *p*-methylcatechol, presumably due to autoxidation.

(3) *p*-Methylcatechol (TP10), identified by comparison to a commercial standard, was detected in reaction mixtures both at pH 3 and 7.

(4) *p*-Benzoquinone, which was detected at pH 7 by comparison of the HPLC retention time and UV/vis spectrum to a standard. This compound could not be detected with mass spectrometry, presumably because the concentration was below the detection limit.

For TP11 and TP14 (Figure 2) extensive information is available, but structural assignment was not unambiguous.

(5) TP11: (a) 3 oxygen atoms were added to the parent mass, (b) one ring deuteron was exchanged for a proton (c) CO₂ loss in the MS data indicated a carboxylic acid, (d) when matched to a peak in the HPLC-DAD chromatogram (Figure S2.1), the suspected peak ($\lambda_{\text{max}} = 266$ nm) was only observed when the aqueous component of the eluent was acidified, which indicated an acidic proton. This peak in the HPLC-DAD chromatogram also appeared as the second main peak upon ozonation of *p*-methylcatechol and (e) the intensity of this peak was dramatically increased in the pH 3 reaction mixture, pointing to a ring-opening product (see mechanistic discussion below). Such a product of *p*-methylcatechol could be formed by ring opening at positions 2–3 or 1–6 (see Figure 2 for numbering of carbons). This would lead to a very polar ring-opening product with both an alcoholic and a carboxylic acid functional group, inconsistent with elution of TP11 only after *p*-methylcatechol. The resulting enol could tautomerize to the corresponding ketone, exhibiting only one hydroxyl/carboxyl group compared to two hydroxyl groups in *p*-methylcatechol, making an elution after *p*-methylcatechol more plausible.

(6) TP14: (a) Addition of one oxygen and loss of two protons compared to the parent, (b) exchange/loss of one ring deuteron, (c) higher yield at pH 7, (d) if matched to the HPLC-DAD chromatogram, this peak ($\lambda_{\text{max}} = 233$ nm) was absent in the *p*-methylcatechol reaction mixture, indicating that TP14 is not a (secondary) metabolite of *p*-methylcatechol, (e) elution after *p*-methylcatechol (should be less polar). A possible structure would correspond to a ring-opening dialdehyde (+2 O) of the parent compound with a subsequent condensation reaction (–H₂O). A ring-opening in the 3–4 position (Figure

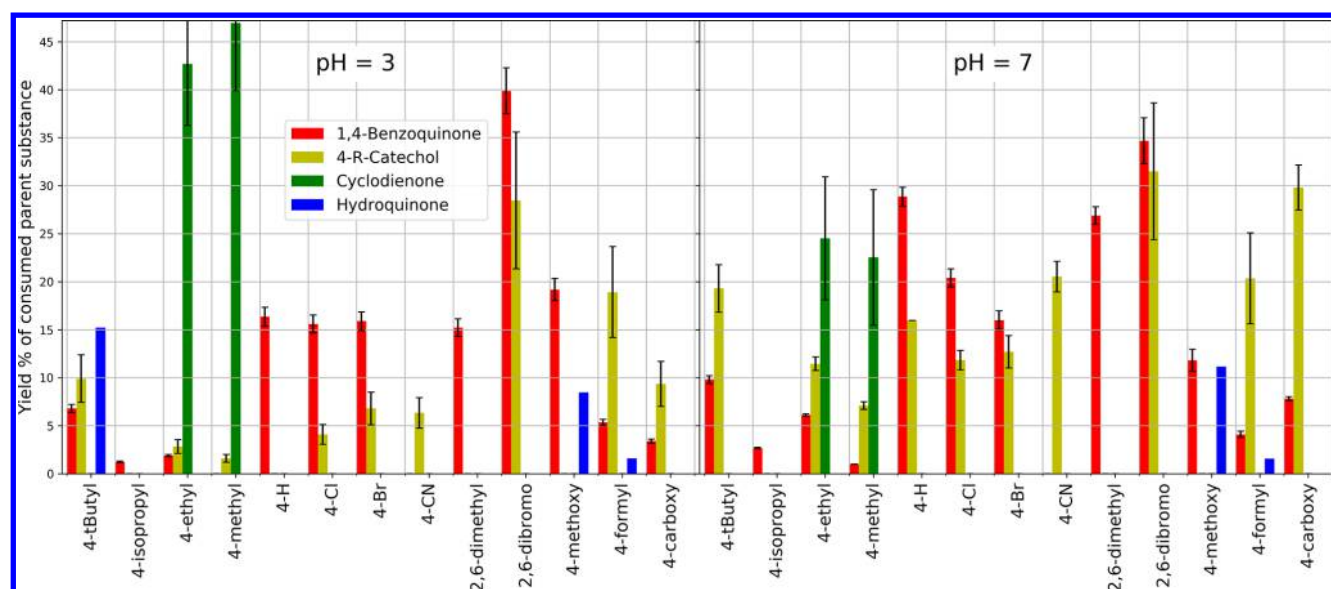


Figure 1. Product yields of (substituted) phenols for the ozonation reactions at a specific ozone dose ($[O_3]/[PhOH]$) of 0.5 at pH 3 or pH 7. For 4-isopropylphenol, the catechol was not quantified. For 2,6-dimethylphenol, no catechol was detected. For 2,6-dibromophenol, catechol could not be unambiguously assigned. Similar data for varying $[O_3]/[PhOH]$, as well as the derivation of experimental uncertainties, are shown in section S6.

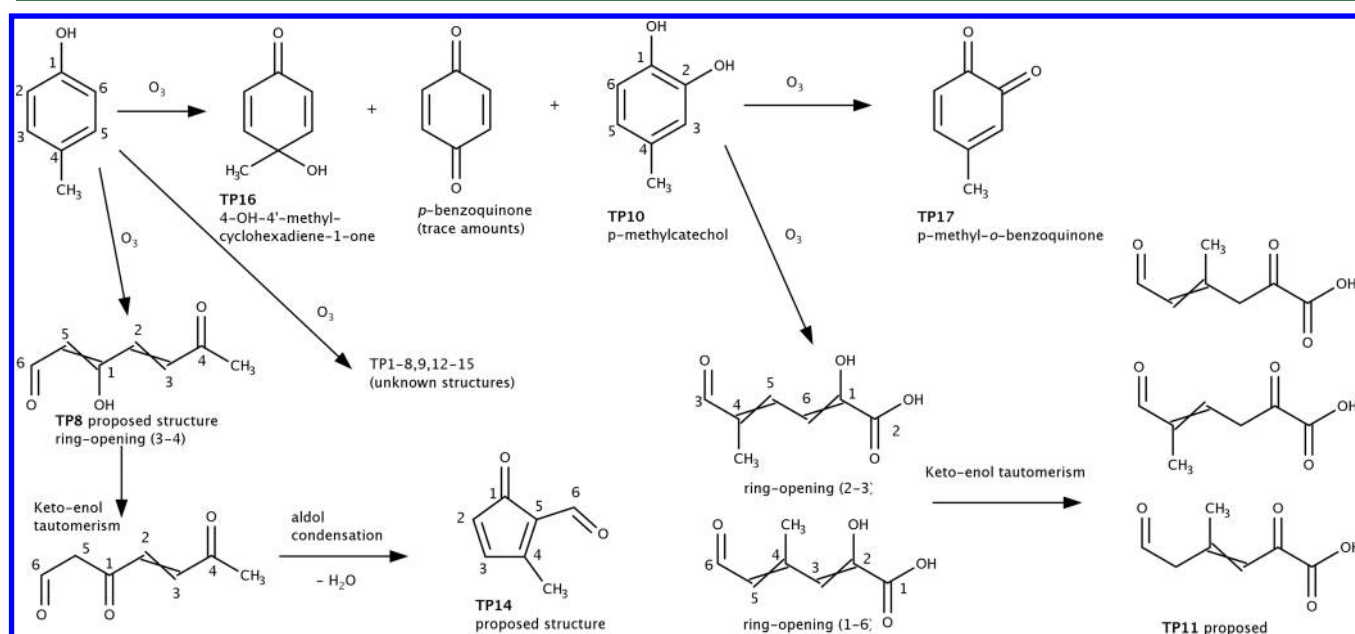


Figure 2. Identified and proposed transformation products in *p*-methylphenol-ozone reaction mixtures. Crossed lines in double bonds indicate unknown stereochemistry. TP10, 16, 17 can be clearly assigned, and structures were proposed for TP11 and TP14.

2), may be followed by a keto–enol tautomerisation and a subsequent aldol condensation to a five-membered ring. Although formation of a ring-opening product is less likely at pH 7, a higher pH could favor the aldol condensation that leads to the proposed structure of TP14.

The remaining 11 products of unknown structures consisted of an addition of 1–4 oxygen atoms to the parent, or oxygen addition with abstraction of two hydrogens (+1–2 O, –2 H) (Table S2). The products should include ring-opening of primary and secondary products, yielding aldehydes and organic acids. Products including the abstraction of two hydrogen atoms could include condensation products as well as quinone/quinoid-type structures. Products in which methyl protons were exchanged/lost were (with one exception) not

observed, which contradicts a previously reported formation of *p*-hydroxy-benzoic acid.⁴⁹ The formation of the latter, as well as *p*-hydroxy-benzaldehyde, was excluded by comparison with commercial standards.

The proposed products encompass many olefinic structures, which are in term rather reactive with ozone ($k \cong 10^3\text{--}10^5\text{ M}^{-1}\text{ s}^{-1}$).¹ However, under wastewater treatment conditions for micropollutant abatement, there is no residual O_3 in the treated water. As different DOM moieties and micropollutants compete for O_3 , first generation oxidation products should only be partially further oxidized and olefinic transformation products might survive.

Tentative Assignment of Analogous Products in Other Reaction Mixtures. The results for *p*-methylphenol are only

Table 2. H₂O₂ Yields (Initial Phenol Concentration 400 μM)^a

	pH 3% O ₃	pH 3% Ph	pH 3: phenol consumption %	pH 7% O ₃	pH 7% Ph	pH 7: phenol consumption %
phenol	36	165	44	18	70	52
<i>p</i> -chlorophenol	15	96	33	8	31	51
<i>p</i> -methylphenol	30	106	69	11	47	55
<i>p</i> -methoxyphenol	16	29	56	12	24	48

^aSpecific ozone doses 0.92–1.03 [O₃]₀/[Phenol]. Yields at pH 3 and pH 7 are given in percentage of ozone consumed (%O₃) or in percentage of parent phenol consumed (%Ph). Phenol consumption refers to the percentage of phenol consumed after O₃ dosage.

partly transferable to other compounds: for 4-alkylated phenols, the observed peaks exhibited the typical optical absorption band of 4-hydroxy-4-alkylcyclohexadienone at ~233 nm, which we confirmed for *p*-ethylphenol with the corresponding synthesized standard. For the 4-alkylphenols provided in Table 1, weak peaks with a band at ~400 nm were observed as well, compatible with the corresponding *o*-benzoquinones. For parent compounds that were not *p*-alkylated, we did not observe peaks with absorption maxima at ~233 nm, indicating the absence of cyclohexadienones (substituents should not influence the spectrum of the cyclohexadienone, as they would not be conjugated to the chromophoric α,β -unsaturated ketone). Only for *p*-methoxyphenol, an intense peak (both at pH 3 and 7) with an absorption maximum at ~420 nm was observed, which is likely the *p*-methoxy-*o*-benzoquinone, discussed below in the context of hydroquinone formation. *o*-Benzoquinones may form from other parent compounds, but may hydrolyze quickly for the electron-poorer parents.

Product Yields. Figure 1 shows the product yields for each compound relative to the consumed parent compound, interpolated for a specific ozone dose ([O₃]₀/[PhOH]₀) of 0.5. These data allow a semiquantitative comparison of product yields between different parent compounds. However, yields can strongly depend on the specific O₃ dose (section S6).

From a kinetic point of view, several trends in yields and phenol consumption can be expected. (1) The catechol yield should decrease with increasing ozone dose, especially at pH 3. Ignoring speciation, catechol is more reactive toward O₃ relative to the parent phenol, at low pH (considering undissociated species) $k(\text{PhOH}) = 1.3 \times 10^3 \text{ M}^{-1} \text{ s}^{-1}$ versus $k(\text{CatOH}) = 5.2 \times 10^5 \text{ M}^{-1} \text{ s}^{-1}$.²³ At pH 7 (considering dissociated species), this difference should be less pronounced: as $k(\text{PhO}^-)$ is already close to the diffusion controlled limit, the (unknown) $k(\text{CatO}^-)$ cannot be 2.5 log(*k*) higher. Catechol yields were found to decrease with increasing ozone doses, with the exception of *p*-halophenols and *p*-carboxyphenol at pH 7.

(2) The *p*-benzoquinone yields should be independent of the ozone dose at pH 7, and could somewhat decrease with increasing ozone dose at pH 3. $k(p\text{-benzoquinone})$ is $2.5 \times 10^3 \text{ M}^{-1} \text{ s}^{-1}$,²² comparable to $k(\text{PhOH})$. At pH 3, there may be competition between these two compounds, whereas at pH 7, the reaction with phenolate will outcompete the reaction with *p*-benzoquinone. A clear decrease in *p*-benzoquinone yield with increasing specific ozone doses at pH 3 was observed for the deactivated phenols (*p*-chloro, *p*-bromo, *p*-formyl, *p*-carboxy), presumably due to a higher extent of consumption of formed *p*-benzoquinone. For *p*-alkylphenols, a slight increase of the *p*-benzoquinone yield with ozone dose was observed, which could hint to the formation of this compound as a secondary product.

(3) The phenol consumption should be lower at pH 3. This effect would be caused by increased reactions of ozone with primary TPs compared to pH 7. This is reasonable not only for catechol, but also for expected ring-opening products, for which

speciation will have a lesser influence on *k*: in this case, the difference between *k*(parent) and *k*(TP) is smaller at pH 3 than at pH 7. Naturally, the phenol consumption should also decrease with increasing ozone/target ratios, as more primary TPs compete with the parent phenol for the remaining ozone. However, in some cases, the phenol consumption was higher at pH 3 (*p*-alkylphenols, *p*-methoxyphenol, 2,6-substituted phenols). The reasons for this behavior remained unclear.

At pH 7, *p*-benzoquinone (red bars in Figure 1) was observed for unsubstituted phenol, *p*-halophenols, and for *p*-methoxyphenol. *p*-Substituted catechols (yellow bars in Figure 1) were detected for all parent compounds except for *p*-methoxyphenol. For *p*-alkylated phenols, the corresponding 4-hydroxy-4-alkylcyclohexadienone was formed instead of *p*-benzoquinone, with only small amounts of the latter in the reaction mixture. Generally, *p*-substitution of the parent phenols did not prevent the attack of O₃ in the *para* position, although the yield can be substantially diminished (e.g., 4-carboxyphenol, 4-formylphenol). Only for 4-cyanophenol, no *p*-benzoquinone was formed.

For the unsubstituted phenol, the yields of *p*-benzoquinone shown in Figure 1 agree well with literature values reported for higher initial phenol concentrations (200–400 μM).^{22,23} These two previous studies differ in their reported catechol yields. Our results support the higher catechol yield reported by Ramseier and von Gunten.²³ However, the catechol yield was rather variable, with results from individual experiments varying between 13% and 20%.

p-Alkylation slightly decreased the catechol yield. This is surprising, as catechol should be a result from an attack of ozone in the ortho position, and *p*-substitution should have little impact on catechol yields. Steric hindering in the *para* position could lead to an increase in catechol yield, but there is no clear dependence of the catechol yield on substituent size either. The formation mechanism of catechols may thus be more complex than previously suggested. No catechol was formed during ozonation of 2,6-dimethylphenol. For 2,6-dibromophenol, 3-bromocatechol may have formed, but owing to overlapping peaks in the chromatogram, it could not be clearly assigned or quantified. Because no standard was available, the *p*-substituted catechol was not quantified for *p*-isopropylphenol. No catechol was detected for *p*-methoxyphenol.

For pH 3, generally somewhat lower yields of *p*-benzoquinone were found (Figure 1) compared to pH 7 for unsubstituted phenol and halophenols. Conversely, the yields of the cyclohexadienones were slightly increased compared to pH 7 and catechol yields were decreased (see discussion above).

H₂O₂ Yields. H₂O₂ is a byproduct of ozonation reactions that arises only from certain reaction mechanisms (e.g., Criegee), and provides further mechanistic insights. H₂O₂ yields were determined for four representative phenols (phenol,

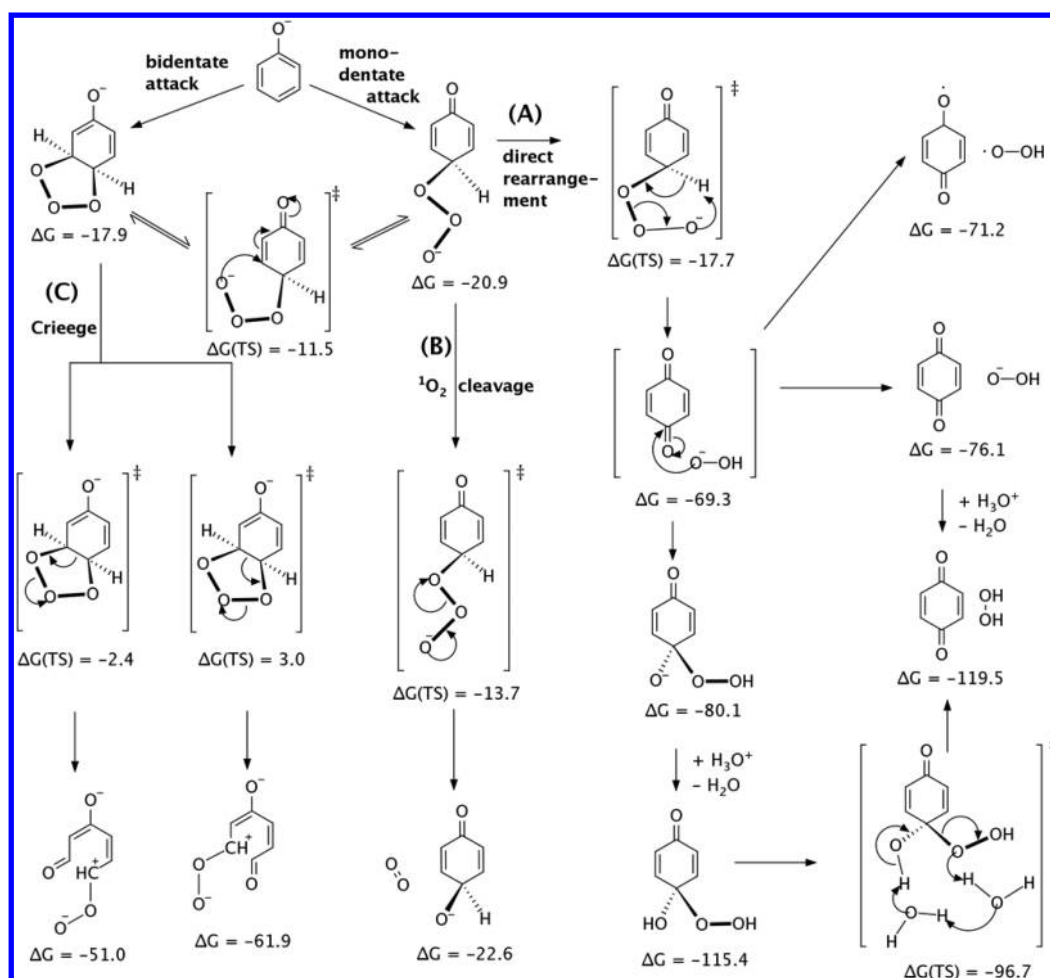


Figure 3. Proposed reaction pathways of unsubstituted phenolate as evaluated by quantum chemical calculations. Reported energies (kcal/mol) are Gibbs' free energies relative to the reactants, computed with the M062X density functional and SMD implicit solvation.

p-chlorophenol, *p*-methylphenol, *p*-methoxyphenol), with an initial concentration of 400 μM (Table 2). At pH 7, the H₂O₂ yield for phenol (18% of consumed O₃) is in good agreement with a previously reported measurement of 16%.²² The yields for *p*-substituted phenols were lower (see discussion below). The H₂O₂ yields at pH 3 were generally much higher than those at pH 7.

Quantum Chemical Calculations and Mechanistic Discussion: Unsubstituted Phenolate. *Mechanistic Considerations Based on Energy Calculations.* As bare O₃ is problematic to common quantum chemical methods,⁵⁰ we performed calculations starting from a monodentate or bidentate adduct of ozone (Figure 3). From these starting points, we considered three different types of reactions: (A) A possible direct rearrangement pathway that could lead to benzoquinone/hydroquinone structures (and H₂O₂) and (B) cleavage of singlet oxygen and (C) cleavage of the double bond (Criegee mechanism) from the cyclic adduct. Given energies may have an uncertainty of several kcal/mol. Nevertheless, these results allow to draw several conclusions: (a) reactant and product structures are connected by transition structures, which shows that these proposed mechanisms are meaningful, (b) evaluation of free energies of reactions shows that all reactions are thermodynamically feasible, and (c) evaluation of reaction barriers can be (cautiously) interpreted to estimate which reaction is kinetically favorable.

Pathways A and B have similarly low reaction barriers and may be favored over pathway C. The cyclic ozonide, which could lead to ring-opening products, is separated by a low barrier from the noncyclic ozonide. Hence, if the initial attack was bidentate, a rearrangement to the noncyclic form should be favored over the ring-opening reaction.

Pathway A leads to an intermediate complex. This complex could be cleaved homolytically (leading to a semiquinone radical) or heterolytically (leading to *p*-benzoquinone and HO₂[−]). Also, this complex could collapse to a dienone-type structure, which could rearrange to *p*-benzoquinone and H₂O₂. An alternative *p*-benzoquinone formation through a cyclic 1–4-ozonide, as also proposed by Mvula and von Sonntag,²² can be excluded based on a much higher computed barrier ($\Delta G^\ddagger > 30$ kcal/mol, not shown).

Formation of Hydrogen Peroxide. Figure 3 shows pathways leading to different reactive oxygen species, with H₂O₂ as a byproduct of *p*-benzoquinone. Other sources of H₂O₂ are Criegee-type reactions opening the aromatic ring, the decay reaction of a product formed by the reaction of *t*-BuOH with [•]OH,⁵¹ and autoxidation of hydroquinone/catechol (which was prevented by acidification of the samples).⁵² Overall, the measured total yield of H₂O₂ at pH 7 was about twice the *p*-benzoquinone yield. Ramseier and von Gunten²³ quantified several noncyclic carboxylic acids during ozonation of phenol, that must have arisen from Criegee-type reactions. They

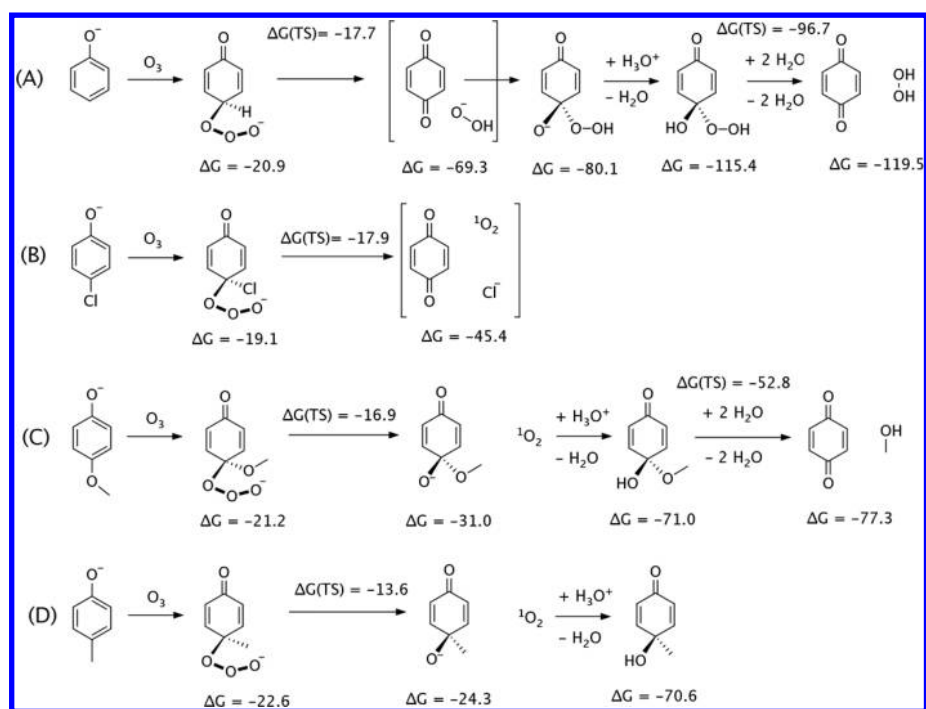


Figure 4. Proposed feasible reaction pathways for the reactions of 4 (substituted) phenolates with ozone, leading either to *p*-benzoquinone or to the cyclohexadienone. Reported energies (kcal/mol) are Gibbs' free energies relative to the reactants, computed with the M062X density functional and SMD implicit solvation.

reported a cumulative yield of these compounds of 31–32% of the consumed phenol at pH 7. When determining the H_2O_2 yield, we used reaction conditions essentially identical to those in Ramseier et al. 2009, yielding 35% of *p*-benzoquinone. In their study, the combined yield of *p*-benzoquinone and the carboxylic acids yield was 66–67%, which can be compared to the present H_2O_2 yield of 70% (Table 2). Another possible source of H_2O_2 is the reaction of $\cdot\text{OH}$ (resulting from electron transfer with phenolate, yield $\sim 13\%$,²² assuming no formaldehyde formation from Criegee reactions) with *t*-BuOH (H_2O_2 yield 30%),⁵¹ which would account for another 4% H_2O_2 in terms of phenol consumed. As the H_2O_2 budget is complete, it is unlikely that the formation of catechol (which we did not investigate mechanistically) also produces H_2O_2 . Calculations (Figure 3) do not support the formation of $\cdot\text{OOH}$ as a byproduct of *p*-benzoquinone, as this is the energetically least favorable pathway.

Quantum Chemical Calculations and Mechanistic Discussion: Unsubstituted Phenol. Mechanistic Considerations Based on Energy Calculations. For the neutral phenol at low pH, detailed quantum chemical calculations were not performed, but some mechanistic considerations are presented in Figure S7.1. In contrast to the phenolate, the monodentate addition of ozone was energetically uphill, owing to the charge separation of the ring and the terminal oxygen of the added ozone. An equilibrium with the cyclic ozonide is unlikely. Instead, the latter is depicted to lead to ring-opening reactions (Criegee mechanism) rather than to equilibrate to the noncyclic ozonide. Thus, bidentate addition as the initial step should lead to Criegee products. The formation of proton-transferred trioxo-species is thermodynamically possible, but would have to proceed through a different mode of initial attack. Any of these reactions could also be in competition with deprotonation of the adduct.

Formation of Hydrogen Peroxide. The H_2O_2 yield (Table 2) at pH 3 was much higher than at pH 7, which indicates a greater importance of ring-opening reactions with H_2O_2 formed through the Criegee mechanism at pH 3. This is corroborated by yields of organic acids and *p*-benzoquinone reported previously under similar reaction conditions.²³ Organic acid yields corresponded to a total H_2O_2 yield of 131%, the benzoquinone yield (assuming H_2O_2 formation also in this case) corresponded to a H_2O_2 yield of 17%. This estimate (total 148%), compares well to a 165% H_2O_2 yield in our experiments. Hence, Criegee-type reactions leading to acidic products are the main source of H_2O_2 . The remaining H_2O_2 could originate from the formation of nonacidic ring-opening products (dialdehydes). We do not expect electron-transfer reactions to contribute to the H_2O_2 budget at pH 3.

Quantum Chemical Calculations and Mechanistic Discussion: Substituted Phenolates. Mechanistic Considerations Based on Energy Calculations. For four representative phenolates (phenolate, *p*-chlorophenolate, *p*-methylphenolate, *p*-methoxyphenolate), we tested the feasibility of different reaction mechanisms leading to *p*-benzoquinone. Similar to Figure 3, the equilibrium between cyclic and noncyclic ozonides was found to be possible. Also, the energetics for singlet oxygen cleavage and the ring-opening reaction did not vary greatly with substitution pattern (data not shown). Clearly, the reaction mechanism leading to *p*-benzoquinone proposed in Figure 3 is not feasible for substituted phenols. Other energetically feasible pathways were found instead, and are summarized in Figure 4.

For *p*-chlorophenolate (Figure 4B), a simultaneous cleavage of chloride and $^1\text{O}_2$ is favorable. A cleavage of $^1\text{O}_2$ only (reaction B in Figure 3) was not found to be possible, leading to the concerted cleavage of chloride instead.

For *p*-methoxyphenolate (Figure 4C), a direct formation of *p*-benzoquinone may be possible after initial cleavage of $^1\text{O}_2$.

The resulting 4-hydroxy-4-methoxy-cyclohexadien-1-one is predicted to easily transfer the hydroxy proton to the methoxy group, yielding methanol and *p*-benzoquinone. Computationally, this reaction is only feasible if catalyzed by explicit water molecules, with a proton transfer to and from these water molecules.

For *p*-methylphenolate (Figure 4D), we did not find a feasible pathway leading to the cleavage of the methyl group, which could lead to *p*-benzoquinone. Of the reactions shown in Figure 3, only channels (B) and (C) can be populated. Of these, $^1\text{O}_2$ release from the noncyclic ozonide is depicted kinetically favorable, leading to the observed product 4-hydroxy-4-methylcyclohexadien-1-one.

Formation of Hydrogen Peroxide. The mechanisms proposed in Figure 4 differ by the type of reactive oxygen species formed. Only for unsubstituted phenolate, there should be production of H_2O_2 along with production of *p*-benzoquinone. The H_2O_2 yield of *p*-chlorophenol is 39% points lower compared to phenol (Table 2). This corresponds roughly to the H_2O_2 yield expected from concurrent formation alongside *p*-benzoquinone from unsubstituted phenol (35%) (Figure 1), which should be lacking for substituted phenols. For *p*-methylphenol, however, the H_2O_2 yield is only 23 percentage points lower compared to phenol (Table 2). Hence, there should be an additional source of H_2O_2 , as the formation of the cyclohexadienone or *p*-benzoquinone from *p*-alkylphenols should not yield H_2O_2 . One possible explanation would be an increase of ring-opening reactions, also producing H_2O_2 , or an increasing contribution of electron transfer reaction for *p*-methylphenol.

$^1\text{O}_2$ yields. Singlet oxygen yields of similar compounds from the literature are compatible with the proposed mechanistic differences between unsubstituted phenol and *p*-chlorophenol, but not with the *p*-methylphenol mechanism. For unsubstituted phenol at pH 7, Mvula and von Sonntag⁴⁰ reported a $^1\text{O}_2$ yield of 5.4% of ozone consumed or 13% of phenol consumed. There are at least two reaction pathways leading to the release of $^1\text{O}_2$. (1) cleavage of singlet oxygen from a primary ozonide, as shown by pathway (B) in Figure 3. In the case of the unsubstituted phenol, this would lead to a cyclohexadienone. This can be expected to rearrange to hydroquinone, a product, which is either absent, or present in very low concentration. However, this product may also have been consumed by secondary reactions with ozone, because of its high reactivity with ozone.²² (2) An initial electron transfer reaction leads to $\text{O}_3^{\cdot-}$ and a phenoxide radical. The former then decomposes to $\cdot\text{OH}$ and $^1\text{O}_2$.¹ In the reaction mixture, $\cdot\text{OH}$ is scavenged by *t*-BuOH, a reaction leading to formaldehyde, which is used for the indirect quantification of $\cdot\text{OH}$. Mvula and von Sonntag²² reported a formaldehyde yield of 12–14% of ozone consumed, formally corresponding to a $\cdot\text{OH}$ yield of 24–28%. However, formaldehyde can also be a terminal product of Criegee-type reactions, which makes a direct assignment of the $\cdot\text{OH}$ yield difficult.

There is no reported data on $^1\text{O}_2$ yield for either *p*-chlorophenol or *p*-methylphenol. For the reaction of analogous pentachloro/pentabromo-phenolate (presumably yielding tetrahalo-*p*-benzoquinone), the $^1\text{O}_2$ yield was found as 58/48% of ozone consumed, whereas the $\cdot\text{OH}$ yield was estimated to be ~27% of ozone consumed.⁴⁰ This supports the presence of pathways leading to singlet oxygen other than electron transfer reactions, compatible with the proposed concerted cleavage of $^1\text{O}_2$ and chloride in *p*-chlorophenol. 2,4,6-Trimethylphenol

should yield cyclohexadienone via $^1\text{O}_2$ cleavage like *p*-methylphenol, but the reported $^1\text{O}_2$ yield is only 10% of O_3 consumed.⁴⁰ This is much lower than the cyclohexadienone yield of *p*-methylphenol reported here.

Mechanistic Discussion: Substituted Phenols. At pH 3, the differences in yields of H_2O_2 between the different parent compounds (Table 2) cannot be rationalized with the reaction schemes proposed above. Except for *p*-methoxyphenol, the H_2O_2 yields are increased compared to pH 7, in agreement with an increased importance of Criegee-type reactions. It remains unclear why this should not be the case for *p*-methoxyphenol.

Mechanistic Discussion of Hydroquinone Formation: Post-ozonation Reactions. Hydroquinone was found as a major product for two parent compounds: (a) *p*-*tert*-butylphenol (only at pH 3) and (b) *p*-methoxyphenol (at both pHs). Hydroquinone is likely not a primary ozonation product, but was formed post-ozonation in the reaction mixture:

(a) For the microbial oxidation of *p*-alkylphenols, 4-hydroxy-4-alkylcyclohexadien-1-ones have been reported as metabolites.^{53–55} Also in this case, hydroquinone was found for a quaternary carbon attached to the aromatic ring. It was proposed that nucleophilic substitution reactions lead to hydroquinone and an alkyl alcohol. Present computations indicate the thermodynamic feasibility for a $\text{S}_{\text{N}}2$ reaction with HO^- (Figure S7.2A and B), and such reactions should be the source of hydroquinone in the present experiments. Hydroquinone was only observed at pH 3. Potentially, in a $\text{S}_{\text{N}}2$ reaction with HO^- , hydroquinone was formed faster at pH 7, and was further oxidized to *p*-benzoquinone by ozone.

(b) For *p*-methoxyphenol, no 4-methoxycatechol was detected, whereas catechols were detected as TPs for all other *p*-substituted parent phenols. The *p*-methoxycatechol probably reacted further in a stepwise process (Figure S7.2C): (1) The reaction of *p*-methoxyphenol to *p*-benzoquinone and *p*-methoxycatechol and (2) a redox cross-reaction between *p*-methoxycatechol and *p*-benzoquinone to yield *p*-methoxy-*o*-benzoquinone and hydroquinone. It was shown previously that dihydroxybenzenes react with *p*-benzoquinones in this way if thermodynamically allowed.⁵⁶ Present thermodynamic calculations depict the reaction as only slightly endergonic, within the uncertainty of calculation (which in this special case of an isodesmic reaction should be <2–3 kcal/mol). An additional experiment, simply mixing standards of *p*-methoxycatechol and *p*-benzoquinone, supports this hypothesis. In this mixture, a new compound was formed, exhibiting an absorption maximum at 420 nm, similar to 4,5-dimethoxy-*o*-benzoquinone⁵⁷ (see Figure S4). This peak was also present in the ozonated reaction mixtures of *p*-methoxyphenol, and was interpreted as *p*-methoxy-*o*-benzoquinone.

Practical Implications. Irrespective of their substitution pattern, ozonation of many electron-rich and electron-poor substituted phenols can contribute to a pool of (substituted) *p*-benzoquinones, cyclohexadienones, catechols, and *o*-benzoquinones. Many phenolic micropollutants contain similar reactive sites as in the present study, including bisphenol A, triclosan, 2-hydroxy-4-methoxybenzophenone, 4-(trifluoromethyl)phenol, chloridazon-desphenyl, 3,5-dibromo-4-hydroxybenzoic acid, *O*-desvenlafaxin, *N,O*-didesvenlafaxin, morphine, mycophenolic acid, neohesperidin dihydrochalcon, naltrexon, deferasirox, albuterol, benserazid, vancomycin, phenylephrine, etc. Additionally, phenolic structures can be found in the background DOM, or can be formed by the reaction of aromatic rings with

hydroxyl radicals that arise during ozonation processes, or from the reaction of ozone with alkoxyaromatics, such as lignins.⁵⁸ The present mechanistic insights can be used for in silico pathway predictions,³⁸ which can be extended to cover substituted phenols.

As shown, post-ozonation reactions can alter the product distributions. In real ozonated waters, a set of initially formed, differently substituted benzoquinones and catechols subsequently relaxes to the thermodynamically most favorable redox speciation: this will generally lead to molecules where electron-donating and electron-withdrawing effects compensate each other, preferring *p*-benzoquinones with electron-donating substituents and hydroquinones or catechols with electron-withdrawing substituents. Especially for (*o/p*-)benzoquinones with electron-withdrawing substituents, such redox reactions may be in competition with reductive hydrolysis. Hydrolyzed products (corresponding trihydroxybenzenes) could then further reduce parent *p*-benzoquinones to hydroquinones (see Figure S5, for examples). Particularly electron-poor benzoquinones hydrolyze quickly: for 2,6-dibromo-1,4-benzoquinone, we observed hydrolysis on the time scale of minutes (hydrolysis before acidification of the sample may also be responsible for the slightly lower benzoquinone yield measured at pH 7 (Figure 1).

Toxicological impact assessment will have to consider a post-ozonation aging of ozonated waters due to redox equilibria, reductive hydrolysis of *o/p*-benzoquinones, and autooxidation of catechols and hydroquinones, as outlined in Figure S5. In treated wastewater, biofiltration will potentially remove many types of formed *p*-benzoquinones by reaction with nucleophiles of biological origin. The products of these types of reactions are increasingly substituted benzoquinones and dihydroxybenzenes, the former becoming less electrophilic with substitution. In drinking water treatment, if ozonation (possibly with biofiltration) is followed by a treatment with chlor(am)ine, the reactions outlined above can influence the formation of disinfection byproducts arising from phenolic moieties, such as chloroform.⁵⁹

■ ASSOCIATED CONTENT

Supporting Information

The Supporting Information is available free of charge on the ACS Publications website at DOI: 10.1021/acs.est.8b00011.

List of standards and reagents, analytical methods, experimental procedures, and additional experimental/modeling data (PDF)

■ AUTHOR INFORMATION

Corresponding Author

*Phone: +41 58 765 5270. Fax: +41 58 765 5802. E-mail: vongunten@eawag.ch.

ORCID

Peter R. Tentscher: 0000-0002-4169-661X

Urs von Gunten: 0000-0001-6852-8977

Notes

The authors declare no competing financial interest.

■ ACKNOWLEDGMENTS

This study was funded by the Swiss National Science Foundation (SNF) project 200021_157143. The authors thank Dr. Samuel Derrer for the synthesis of 4-OH-4-

alkylcyclohexadienones and technical support, and Elisabeth Sahli, Ursula Schönenberger, and Sung Eun Lim for technical support.

■ REFERENCES

- (1) von Gunten, U.; von Sonntag, C. *Chemistry of Ozone in Water and Wastewater Treatment*; IWA Publishing, 2012.
- (2) Hollender, J.; Zimmermann, S. G.; Koepke, S.; Krauss, M.; McArdell, C. S.; Ort, C.; Singer, H.; von Gunten, U.; Siegrist, H. Elimination of Organic Micropollutants in a Municipal Wastewater Treatment Plant Upgraded with a Full-Scale Post-Ozonation Followed by Sand Filtration. *Environ. Sci. Technol.* **2009**, *43* (20), 7862–7869.
- (3) Huber, M. M.; Gobel, A.; Joss, A.; Hermann, N.; Löffler, D.; McArdell, C. S.; Ried, A.; Siegrist, H.; Ternes, T. A.; von Gunten, U. Oxidation of pharmaceuticals during ozonation of municipal wastewater effluents: A pilot study. *Environ. Sci. Technol.* **2005**, *39* (11), 4290–4299.
- (4) Lee, Y.; Gerrity, D.; Lee, M.; Bogeat, A. E.; Salhi, E.; Gamage, S.; Trenholm, R. A.; Wert, E. C.; Snyder, S. A.; von Gunten, U. Prediction of Micropollutant Elimination during Ozonation of Municipal Wastewater Effluents: Use of Kinetic and Water Specific Information. *Environ. Sci. Technol.* **2013**, *47* (11), 5872–5881.
- (5) Lee, Y.; Kovalova, L.; McArdell, C. S.; von Gunten, U. Prediction of micropollutant elimination during ozonation of a hospital wastewater effluent. *Water Res.* **2014**, *64*, 134–148.
- (6) Bourgin, M.; Beck, B.; Boehler, M.; Borowska, E.; Fleiner, J.; Salhi, E.; Teichler, R.; von Gunten, U.; Siegrist, H.; McArdell, C. S. Evaluation of a full-scale wastewater treatment plant upgraded with ozonation and biological post-treatments: Abatement of micropollutants, formation of transformation products and oxidation by-products. *Water Res.* **2018**, *129*, 486–498.
- (7) Chon, K.; Salhi, E.; von Gunten, U. Combination of UV absorbance and electron donating capacity to assess degradation of micropollutants and formation of bromate during ozonation of wastewater effluents. *Water Res.* **2015**, *81*, 388–397.
- (8) Hubner, U.; von Gunten, U.; Jekel, M. Evaluation of the persistence of transformation products from ozonation of trace organic compounds - A critical review. *Water Res.* **2015**, *68*, 150–170.
- (9) Huber, M. M.; Ternes, T. A.; von Gunten, U. Removal of estrogenic activity and formation of oxidation products during ozonation of 17 alpha-ethinylestradiol. *Environ. Sci. Technol.* **2004**, *38* (19), 5177–5186.
- (10) Dodd, M. C.; Rentsch, D.; Singer, H. P.; Kohler, H. P. E.; von Gunten, U. Transformation of beta-lactam Antibacterial Agents during Aqueous Ozonation: Reaction Pathways and Quantitative Bioassay of Biologically-Active Oxidation Products. *Environ. Sci. Technol.* **2010**, *44* (22), 8790–8790.
- (11) Mawhinney, D. B.; Vanderford, B. J.; Snyder, S. A. Transformation of 1H-Benzotriazole by Ozone in Aqueous Solution. *Environ. Sci. Technol.* **2012**, *46* (13), 7102–7111.
- (12) Mestankova, H.; Parker, A. M.; Bramaz, N.; Canonica, S.; Schirmer, K.; von Gunten, U.; Linden, K. G. Transformation of Contaminant Candidate List (CCL3) compounds during ozonation and advanced oxidation processes in drinking water: Assessment of biological effects. *Water Res.* **2016**, *93*, 110–120.
- (13) Sein, M. M.; Zedda, M.; Tuerk, J.; Schmidt, T. C.; Gollock, A.; von Sonntag, C. Oxidation of diclofenac with ozone in aqueous solution. *Environ. Sci. Technol.* **2008**, *42* (17), 6656–6662.
- (14) Lee, Y.; Escher, B. I.; Von Gunten, U. Efficient removal of estrogenic activity during oxidative treatment of waters containing steroid estrogens. *Environ. Sci. Technol.* **2008**, *42* (17), 6333–6339.
- (15) Mestankova, H.; Schirmer, K.; Escher, B. I.; von Gunten, U.; Canonica, S. Removal of the antiviral agent oseltamivir and its biological activity by oxidative processes. *Environ. Pollut.* **2012**, *161*, 30–35.
- (16) Lange, F.; Cornelissen, S.; Kubac, D.; Sein, M. M.; von Sonntag, J.; Hannich, C. B.; Gollock, A.; Heipieper, H. J.; Moder, M.; von Sonntag, C. Degradation of macrolide antibiotics by ozone: A

mechanistic case study with clarithromycin. *Chemosphere* **2006**, *65* (1), 17–23.

(17) Vanwelie, R. T. H.; Vandijck, R. G. J. M.; Vermeulen, N. P. E.; Vansittert, N. J. Mercapturic Acids, Protein Adducts, and DNA Adducts as Biomarkers of Electrophilic Chemicals. *Crit. Rev. Toxicol.* **1992**, *22* (5–6), 271–306.

(18) Benigni, R.; Bossa, C. Mechanisms of chemical carcinogenicity and mutagenicity: a review with implications for predictive toxicology. *Chem. Rev.* **2011**, *111* (4), 2507–36.

(19) Gold, L. S. The Carcinogenic Potency Database (CPDB). <https://toxnet.nlm.nih.gov/cpdb/> (accessed December 2017).

(20) Gold, L. S.; Manley, N. B.; Slone, T. H.; Rohrbach, L. Supplement to the Carcinogenic Potency Database (CPDB): Results of animal bioassays published in the general literature in 1993 to 1994 and by the National Toxicology Program in 1995 to 1996. *Environ. Health Persp.* **1999**, *107*, 527.

(21) Gold, L. S.; Manley, N. B.; Slone, T. H.; Rohrbach, L.; Garfinkel, G. B. Supplement to the Carcinogenic Potency Database (CPDB): Results of animal bioassays published in the general literature through 1997 and by the National Toxicology Program in 1997–1998. *Toxicol. Sci.* **2005**, *85* (2), 747–808.

(22) Mvula, E.; von Sonntag, C. Ozonolysis of phenols in aqueous solution. *Org. Biomol. Chem.* **2003**, *1* (10), 1749–56.

(23) Ramseier, M. K.; von Gunten, U. Mechanisms of Phenol Ozonation-Kinetics of Formation of Primary and Secondary Reaction Products. *Ozone: Sci. Eng.* **2009**, *31* (3), 201–215.

(24) Gotz, C. W.; Stamm, C.; Fenner, K.; Singer, H.; Scharer, M.; Hollender, J. Targeting aquatic microcontaminants for monitoring: exposure categorization and application to the Swiss situation. *Environ. Sci. Pollut. Res.* **2010**, *17* (2), 341–54.

(25) von Sonntag, C. Degradation of aromatics by Advanced Oxidation Processes in water remediation: Some basic considerations. *J. Water Supply Res. T.* **1996**, *45* (2), 84–91.

(26) von Sonntag, C.; Dowideit, P.; Fang, X. W.; Mertens, R.; Pan, X. M.; Schuchmann, M. N.; Schuchmann, H. P. The fate of peroxy radicals in aqueous solution. *Water Sci. Technol.* **1997**, *35* (4), 9–15.

(27) International Humic Substances Society. <http://humic-substances.org> (accessed December 2017).

(28) Ma, H. Z.; Allen, H. E.; Yin, Y. J. Characterization of isolated fractions of dissolved organic matter from natural waters and a wastewater effluent. *Water Res.* **2001**, *35* (4), 985–996.

(29) Deborde, M.; Rabouan, S.; Mazellier, P.; Duguet, J. P.; Legube, B. Oxidation of bisphenol A by ozone in aqueous solution. *Water Res.* **2008**, *42* (16), 4299–308.

(30) Lau, T. K.; Chu, W.; Graham, N. Reaction pathways and kinetics of butylated hydroxyanisole with UV, ozonation, and UV/O₃ processes. *Water Res.* **2007**, *41* (4), 765–774.

(31) Pi, Y.; Zhang, L.; Wang, J. The formation and influence of hydrogen peroxide during ozonation of *para*-chlorophenol. *J. Hazard. Mater.* **2007**, *141* (3), 707–12.

(32) Trapido, M.; Veressina, Y.; Hentunen, J. K.; Hirvonen, A. Ozonation of chlorophenols: Kinetics, by-products and toxicity. *Environ. Technol.* **1997**, *18* (3), 325–332.

(33) Andreozzi, R.; Caprio, V.; Marotta, R.; Vogna, D. Paracetamol oxidation from aqueous solutions by means of ozonation and H₂O₂/UV system. *Water Res.* **2003**, *37* (5), 993–1004.

(34) Shang, N. C.; Yu, Y. H.; Ma, H. W.; Chang, C. H.; Liou, M. L. Toxicity measurements in aqueous solution during ozonation of mono-chlorophenols. *J. Environ. Manage.* **2006**, *78* (3), 216–22.

(35) Ning, B.; Graham, N. J. D.; Zhang, Y. Degradation of octylphenol and nonylphenol by ozone textendash Part I: Direct reaction. *Chemosphere* **2007**, *68* (6), 1163–1172.

(36) Pillar, E. A.; Camm, R. C.; Guzman, M. I. Catechol oxidation by ozone and hydroxyl radicals at the air-water interface. *Environ. Sci. Technol.* **2014**, *48* (24), 14352–60.

(37) Staehelin, J.; Hoigne, J. Decomposition of Ozone in Water in the Presence of Organic Solutes Acting as Promoters and Inhibitors of Radical Chain Reactions. *Environ. Sci. Technol.* **1985**, *19* (12), 1206–1213.

(38) Lee, M.; Blum, L. C.; Schmid, E.; Fenner, K.; von Gunten, U. A computer-based prediction platform for the reaction of ozone with organic compounds in aqueous solution: kinetics and mechanisms. *Environ. Sci.-Proc. Imp.* **2017**, *19* (3), 465–476.

(39) Held, A. M.; Halko, D. J.; Hurst, J. K. Mechanisms of Chlorine Oxidation of Hydrogen-Peroxide. *J. Am. Chem. Soc.* **1978**, *100* (18), 5732–5740.

(40) Munoz, F.; Mvula, E.; Braslavsky, S. E.; von Sonntag, C. Singlet dioxygen formation in ozone reactions in aqueous solution. *J. Chem. Soc. Perk T 2* **2001**, No. 7, 1109–1116.

(41) Zhao, Y.; Truhlar, D. G. The M06 suite of density functionals for main group thermochemistry, thermochemical kinetics, non-covalent interactions, excited states, and transition elements: two new functionals and systematic testing of four M06-class functionals and 12 other functionals. *Theor. Chem. Acc.* **2008**, *120* (1–3), 215–241.

(42) Peverati, R.; Truhlar, D. G. Improving the Accuracy of Hybrid Meta-GGA Density Functionals by Range Separation. *J. Phys. Chem. Lett.* **2011**, *2* (21), 2810–2817.

(43) Montgomery, J. A.; Frisch, M. J.; Ochterski, J. W.; Petersson, G. A. A complete basis set model chemistry. VII. Use of the minimum population localization method. *J. Chem. Phys.* **2000**, *112* (15), 6532–6542.

(44) Boyle, E. S.; Guerriero, N.; Thiallet, A.; Del Vecchio, R.; Blough, N. V. Optical Properties of Humic Substances and CDOM: Relation to Structure. *Environ. Sci. Technol.* **2009**, *43* (7), 2262–2268.

(45) Hoigne, J.; Bader, H. Rate Constants of Reactions of Ozone with Organic and Inorganic-Compounds in Water 0.2. Dissociating Organic-Compounds. *Water Res.* **1983**, *17* (2), 185–194.

(46) Benigni, R.; Bossa, C.; Tcheremenskaia, O. Nongenotoxic Carcinogenicity of Chemicals: Mechanisms of Action and Early Recognition through a New Set of Structural Alerts. *Chem. Rev.* **2013**, *113* (5), 2940–2957.

(47) Albarran, G.; Boggess, W.; Rassolov, V.; Schuler, R. H. Absorption spectrum, mass spectrometric properties, and electronic structure of 1,2-benzoquinone. *J. Phys. Chem. A* **2010**, *114* (28), 7470–8.

(48) Criquet, J.; Rodriguez, E. M.; Allard, S.; Wellauer, S.; Salhi, E.; Joll, C. A.; von Gunten, U. Reaction of bromine and chlorine with phenolic compounds and natural organic matter extracts - Electrophilic aromatic substitution and oxidation. *Water Res.* **2015**, *85*, 476–486.

(49) Valsania, M. C.; Fasano, F.; Richardson, S. D.; Vincenti, M. Investigation of the degradation of cresols in the treatments with ozone. *Water Res.* **2012**, *46* (8), 2795–804.

(50) Zhao, Y.; Tishchenko, O.; Gour, J. R.; Li, W.; Lutz, J. J.; Piecuch, P.; Truhlar, D. G. Thermochemical Kinetics for Multireference Systems: Addition Reactions of Ozone. *J. Phys. Chem. A* **2009**, *113* (19), 5786–5799.

(51) Acero, J. L.; von Gunten, U. Influence of carbonate on the ozone/hydrogen peroxide based advanced oxidation process for drinking water treatment. *Ozone: Sci. Eng.* **2000**, *22* (3), 305–328.

(52) La Mer, V. K.; Rideal, E. K. The influence of hydrogen concentration on the auto-oxidation of hydroquinone. A note on the stability of the quinhydrone electrode. *J. Am. Chem. Soc.* **1924**, *45*, 223–231.

(53) Gabriel, F. L.; Cyris, M.; Jonkers, N.; Giger, W.; Guenther, K.; Kohler, H. P. Elucidation of the ipso-substitution mechanism for side-chain cleavage of alpha-quaternary 4-nonylphenols and 4-*t*-butoxyphenol in *Sphingobium xenophagum* Bayram. *Appl. Environ. Microbiol.* **2007**, *73* (10), 3320–6.

(54) Gabriel, F. L.; Giger, W.; Guenther, K.; Kohler, H. P. Differential degradation of nonylphenol isomers by *Sphingomonas xenophaga* Bayram. *Appl. Environ. Microbiol.* **2005**, *71* (3), 1123–9.

(55) Gabriel, F. L. P.; Cyris, M.; Giger, W.; Kohler, H.-P. E. ipso-Substitution: A General Biochemical and Biodegradation Mechanism to Cleave-Quaternary Alkylphenols and Bisphenol A. *Chem. Biodiversity* **2007**, *4* (9), 2123–2137.

- (56) Uchimiya, M.; Stone, A. T. Aqueous oxidation of substituted dihydroxybenzenes by substituted benzoquinones. *Environ. Sci. Technol.* **2006**, *40* (11), 3515–21.
- (57) Volod'ko, L. V.; Komyak, A. I.; Min'ko, A. A.; Tatarinov, B. A.; Matusevich, P. A. Electronic Absorption of Spectra of Some o-Benzoquinone Derivatives. *Zhurnal Prikladnoi Spektroskopii* **1976**, *24* (6), 1009–1014.
- (58) Mvula, E.; Naumov, S.; von Sonntag, C. Ozonolysis of lignin models in aqueous solution: anisole, 1,2-dimethoxybenzene, 1,4-dimethoxybenzene, and 1,3,5-trimethoxybenzene. *Environ. Sci. Technol.* **2009**, *43* (16), 6275–82.
- (59) Gallard, H.; Von Gunten, U. Chlorination of phenols: Kinetics and formation of chloroform. *Environ. Sci. Technol.* **2002**, *36* (5), 884–890.
- (60) Liptak, M. D.; Gross, K. C.; Seybold, P. G.; Feldgus, S.; Shields, G. C. Absolute pK(a) determinations for substituted phenols. *J. Am. Chem. Soc.* **2002**, *124* (22), 6421–6427.
- (61) Svobodova Varekova, R.; Geidl, S.; Ionescu, C. M.; Skrehota, O.; Kudera, M.; Sehnal, D.; Bouchal, T.; Abagyan, R.; Huber, H. J.; Koca, J. Predicting pK(a) values of substituted phenols from atomic charges: comparison of different quantum mechanical methods and charge distribution schemes. *J. Chem. Inf. Model.* **2011**, *51* (8), 1795–806.